Pressure-Dependent NMR Spectroscopy Indicates That Internal Rotation of Gas-Phase Formamide Follows Statistical Kinetics

Angela N. Taha and Nancy S. True*

Department of Chemistry, University of California, One Shields Avenue, Davis, California 95616

Received: May 3, 2000; In Final Form: July 20, 2000

Pressure-dependent internal rotation rate constants for [^{15}N]formamide in gas mixtures containing 1.3 Torr of [^{15}N]formamide and SF_6 pressures ranging from 150 to 5225 Torr were determined from analysis of exchange-broadened ^{1}H NMR spectra obtained at 333 K. They agree well with RRKM calculations using experimental vibrational frequencies and rotational constants for the ground state and appropriately scaled 6-311++G** parameters for the transition states. The strong collision model, with a hard sphere diameter of 4.8 Å, yields satisfactory agreement. Activated formamide molecules have an average calculated energy specific rate constant, $\langle k(E)\rangle$, of ca. 5.3×10^9 s^{-1} and a state density of ca. 7.2 cm^{-1}. Statistical internal rotation kinetics requires activated formamide molecules to have vibrational lifetimes of <200 ps and average intervibrational coupling matrix elements of ≥ 0.1 cm^{-1}. These results are compared to kinetic studies of similar low-energy unimolecular processes.

Introduction

Formamide (FA), the simplest molecule containing the amide linkage, undergoes internal rotation on a time scale that is accessible to measurement by NMR spectroscopy. Most NMR studies of FA internal rotation have been performed using condensed-phase samples, and little is known about the gas-phase kinetics of this process. We recently reported the gas-phase activation energy [$E_\infty = 16.6(0.3)$ kcal mol^{-1}] for internal rotation of FA,[1] which is close to the most recently reported theoretical value (15.8 kcal mol^{-1}) calculated at the CCSD(T) electron correlation level using a PVTZ basis set.[2] Our initial studies found that the internal rotation rate constant of FA is pressure-dependent over a large pressure range and appears to be in the unimolecular limit when ca. 3000 Torr of SF_6 is present. Pressure-dependent rate constants of unimolecular processes can provide information about intramolecular dynamics. FA is the only amide that we have studied in the gas phase which displays pressure-dependent internal rotation rate constants at experimentally accessible pressures. All the previously studied amides are larger than FA, and their internal rotation rate constants are independent of pressure at pressures above a few Torr.[3,4] This study of FA internal rotation addresses the question of whether this process follows statistical kinetics.

Although rate constants of many low-energy conformational processes have been analyzed within the framework of transition state (TS) theory,[5] these processes may not always be statistical. Statistical kinetic theories such as TS theory and, in the gas phase, Rice−Ramsperger−Kassel−Marcus (RRKM) theory implicitly assume ergodic intramolecular vibrational redistribution (IVR) on a time scale that is faster than the reaction time.[6] The validity of this assumption depends on factors such as molecular size and structure, barrier height, symmetry restrictions, initial state preparation, and environment. Unimolecular reactions can exhibit intrinsic non-RRKM behavior arising from inherently weak coupling between the vibrational modes of a molecule. Intrinsic non-RRKM behavior is possible if the reactant has structural or symmetry restrictions which impede internal energy flow and is more likely for processes which occur at low energies where vibrational coupling is weak. Whether a process is statistical or not can also depend on initial state preparation. Hase and Bunker defined a second type of non-RRKM behavior, apparent non-RRKM behavior, which arises from the capability of rapid reaction before energy randomization can occur.[7] Apparent non-RRKM behavior can occur when a molecule is prepared in an excited state well above the reaction barrier, where the energy specific rate constant, $k(E)$, in the statistical limit is rapid compared to IVR rate constants, k_{IVR}s, at that energy.

For the conformational processes which have been studied to date, the requirement for statistical kinetics, i.e., that $k_{IVR} > k(E)$, appears to be met when the RRKM-calculated $k(E)$s are less than ca. 10^9 s^{-1} but not when the RRKM-calculated $k(E)$ is ca. $\geq 10^{12}$ s^{-1}. Pressure-dependent rate constants of 14 thermally initiated low-energy conformational processes studied in our laboratory, including internal rotations, ring inversions, and pseudorotations, obtained from analysis of exchange-broadened NMR spectra are consistent with RRKM predictions.[8−21] In all these studies, rate constants were measured near 300 K where the internal energy of most of the activated molecules was less than 1 kcal mol^{-1} above the threshold energy for the process. Table 1 lists threshold energies (E_0), state densities for the activated molecules at E_0 [$\rho(E_0)$], and average energy specific rate constants [$\langle k(E)\rangle$], for these processes. The $\langle k(E)\rangle$s for the molecules listed in Table 1 ranged from 2×10^9 s^{-1} for methyl nitrite internal rotation to 3×10^5 s^{-1} for ring inversion in trimethylhexahydrotriazine. In contrast, conformational isomerization of allyl fluoride[22,23] and 2-fluoroethanol[24,25] which occurred after the molecules were excited to a C−H $v = 1$ zero-order bright state (ZOBS) at internal energies roughly 3 times the threshold energy was several orders of magnitude slower than predicted by RRKM theory. In these studies, the RRKM-calculated $k(E)$s were ca. 10^{12} s^{-1}, several orders of magnitude larger than those of the fastest processes listed in Table 1.

On the basis of these results, it is likely that conformational processes with RRKM-calculated $k(E)$s between 10^9 and 10^{12}

10.1021/jp001666i CCC: $19.00
Published on Web 08/24/2000

TABLE 1: Threshold Energies (E_0), State Densities $\rho(E_0)$, and Approximate Average Energy Specific Rate Constants, $\langle k(E)\rangle$, of Molecules Undergoing Low-Energy Processes

process	E_0 (kcal mol^{-1})	$\rho(E_0)$ (states cm^{-1})	$\langle k(E)\rangle$ (s^{-1})
internal rotation			
methyl nitrite (syn)[a]	12.8(0.2)	3.4×10^1	2.6×10^9
ethyl nitrite (syn)[b]	11.6(0.4)	4.0×10^2	1.2×10^9
n-propyl nitrite (syn)[b]	11.8(0.2)	1.7×10^5	1.6×10^8
n-butyl nitrite (syn)[b]	11.6(0.2)	6.9×10^5	2.8×10^7
formamide[c]	16.4(0.3)	7.2×10^0	5.3×10^9
ring inversion			
cyclohexane[d]	12.6	1.5×10^3	2.0×10^9
cyclohexyl fluoride[e]	11.6	3.1×10^3	3.7×10^9
tetrahydropyran[f]	12.1	7.0×10^2	3.5×10^9
N-methylmorpholine[g]	12.3	9.8×10^3	9.6×10^7
N,*N*-dimethylpiperazine[h]	14.8	1.3×10^6	3.0×10^7
1,3,5-trimethylhexahydro-1,3,5-triazine[i]	13.3	5.9×10^6	3.0×10^5
N-methylpiperidine[j]	12.4	2.4×10^4	9.3×10^7
N-methylpiperazine[k]	12.8	1.8×10^4	8.2×10^7
pseudorotation			
sulfur tetrafluoride[l]	11.8(0.2)	4.8×10^1	7.4×10^8
bullvalene[m]	13.2(0.2)	1.7×10^4	5.7×10^6

[a] From refs 8 and 9. [b] From ref 10. [c] This work. [d] From ref 11. [e] From ref 12. [f] From ref 13. [g] From ref 14. [h] From ref 15. [i] From ref 16. [j] From ref 17. [k] From ref 18. [l] From refs 19 and 20. [m] From ref 21.

s^{-1} will show some departure from statistical kinetics. The calculated $\langle k(E)\rangle$ for FA, ca. 5×10^9 s^{-1}, is faster than that of any of the previously studied thermally initiated conformational processes, and corresponding faster IVR rate constants are required for statistical kinetics. The highly coupled nature of the reaction coordinate which describes the internal rotation of FA and is discussed below may facilitate IVR in activated FA molecules.

Conformational isomerization in many molecules is adequately represented as a one-dimensional internal rotation process. Internal rotation in FA is more complex. The hybridization of the nitrogen atom changes from sp^2 in the ground state to sp^3 at the two possible transition states, TS1 (nitrogen lone pair axis syn to the formyl proton) and TS2 (nitrogen lone pair axis syn to the carbonyl oxygen). TS1 and TS2 are predicted to have energies 16.69 and 19.30 kcal mol^{-1} higher than that of the ground state, respectively, at the MP2/6-31G* level of theory.[26] The minimum energy interconversion path involves both torsional motion and nitrogen inversion. Figure 1 shows structures along the reaction path corresponding to motion of the N lone pair axis from its equilibrium position, orthogonal to the molecular plane to a position where it is in the CON plane syn to the carbonyl oxygen (TS2) with concurrent rehybridization of the N atom. Calculations were performed with one O−C−N−H torsional angle constrained at the value given below each structure. As the value of the constrained torsional angle increases, the nitrogen atom develops more sp^3 character and the distance between the two amino protons decreases to a minimum at the 120° structure (TS2). The alternate reaction path involves rotation of the N lone pair axis from its equilibrium orthogonal position to a position where it is in the C−O−N plane anti to the carbonyl (TS1), also with concurrent rehybridization. The out-of-plane N−H vibrations of FA are strongly coupled. Recently, calculations at the MP2/6-311G** level were used to construct a potential energy surface for FA as a function of two internal coordinates which mimic the inversion and internal rotation modes. The calculated vibrational frequencies for the coupled inversion and internal rotation agree more closely with the experimentally determined values than do vibrational frequencies calculated using uncoupled one-dimensional potential functions for each vibration.[27]

This study reports internal rotation rate constants of FA as a function of total system pressure and compares them to statistical predictions. Ab initio molecular orbital calculations were performed to aid in determining structural and vibrational parameters for use in kinetic modeling. The satisfactory agreement between experimental and calculated rate constants and its implications are described. Results are compared to previously studied conformational processes which were thermally

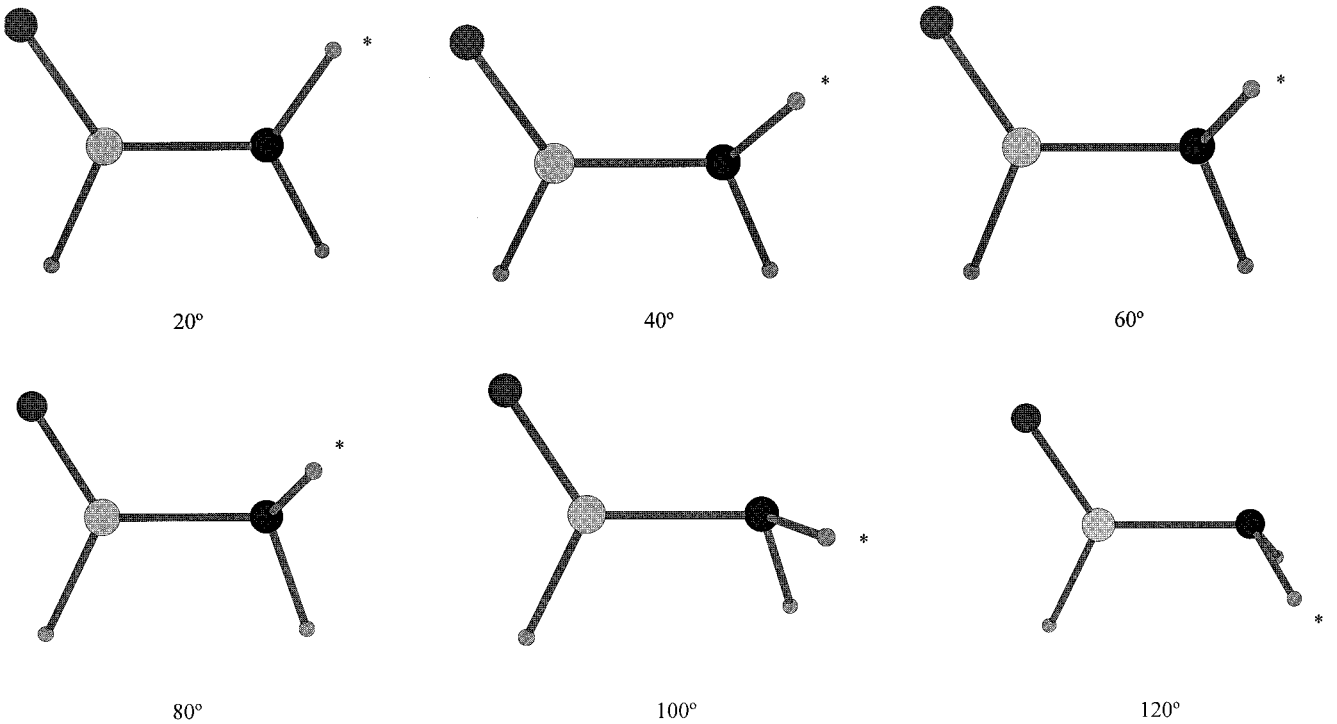

Figure 1. Minimum energy structures (HF/6-31G**) of FA with one O−C−N−H torsional angle constrained at the values shown. The torsional angles are accurately illustrated. The N−H that was constrained is marked with an asterisk.

TABLE 2: Parameters for RRKM Calculations for [^{15}N]Formamide

vibrational frequencies (cm^{-1})	ground state		TS1	TS2
	experimental	calculated[a]	calculated[a]	calculated[a]
A′	599.2, 551.0, 1298.8, 1390.4, 1600.6, 1688.9, 2764.4, 3295.0, 3412.4	668, 615, 1365, 1552, 1779, 1965, 3225, 3823, 3953	642, 982, 1183, 1525, 1742, 2000, 3194, 3693	639, 989, 1198, 1539, 1748, 2029, 3220, 3704
A″	266.0, 1049.6, 1021.2	228, 1176, 1148	958, 1362, 3759	959, 1366, 3779
rotational constants[b] (GHz)				
A	72.448	75.070	65.871	65.566
B	11.054	11.277	10.921	10.907
C	9.589	9.804	9.842	9.821

[a] Unscaled vibrational frequencies calculated at 298 K at the HF/6-311++G** level of theory. [b] From ref 34.

initiated or where the reactive population was prepared in a single vibrationally excited state at an energy well in excess of the threshold energy required for the process.

Experimental Procedures

Sample Preparation. Gas-phase FA/SF_6 samples were prepared in restricted-volume NMR tubes constructed from 3 cm long sections of Wilmad high-precision 12 mm o.d. coaxial inserts. All samples contained 1.3 Torr of [^{15}N]FA (Isotec, Inc., 99% pure), 10−20 Torr of TMS, and SF_6 at pressures ranging from 150 to 5225 Torr at 333 K. [^{15}N]FA was used to avoid line broadening from quadrupolar relaxation.[1] The samples were prepared by deposition of a small amount of liquid [^{15}N]FA in the bottom of the insert tube. The sample tubes were then attached to a vacuum manifold for introduction of bath and reference gases. All pressure measurements were taken with an MKS capacitance manometer with a 1000 Torr head and digital readout. Each sample was made by quantitatively transferring a mixture of measured partial pressures of SF_6 and TMS from a calibrated glass bulb into an insert tube. Cooled samples were torch sealed and immersed in liquid nitrogen. Final sample pressures were calculated using the ideal gas law and are corrected for any residual pressure in the vacuum line after sealing the sample. Samples with total pressures of >3500 Torr were similarly prepared in 12 mm o.d. heavy-walled Wilmad NMR tubes. Uncertainty in the final sample pressures arises primarily from uncertainties in the final volume of the sample due to the sealing technique and is estimated to be 1%.

Total sample pressures corrected for the temperature at which rate constants were measured, 333 K, are listed in Table 3. Intensity measurements of the FA resonances indicated that the partial pressure of FA in each sample was constant at 1.3 Torr at 333 K.

NMR Spectroscopy and Rate Constants. Gas-phase NMR spectra of [^{15}N]FA were acquired with a wide-bore GE NT-300 NMR spectrometer fitted with a Tecmag acquisition upgrade and equipped with a Bradley 12 mm ^{1}H probe. All measurements were taken on spinning samples in the unlocked mode. Acquisition parameters were as follows: pulse length, 14 μs (90° flip angle); delay time, 2 s; and acquisition time, 1.6 s. Longer delay times (4 s) did not result in any changes in the pressure-dependent spectra at low (250 and 472 Torr), intermediate (796 and 1041 Torr), and high pressures (3462 Torr). Typically, 25 000 transients were collected and stored in 8K of memory to achieve a maximum signal-to-noise ratio of 10:1 after multiplication by an exponential line broadening factor of 1 Hz. A sweep width of 2500 Hz was employed. The temperature was controlled to ±0.1 °C and read after each acquisition. Temperature measurements were taken using two copper−constantan thermocouples placed within an empty NMR tube. Using this technique, the temperature gradient within the active volume of the probe was found to be less than 0.2 K. Samples were allowed to thermally equilibrate for at least 10 min prior to sample acquisition.

TABLE 3: Internal Rotation Rate Constants of FA as a Function of Total System Pressure at 333 K (Uncertainties of 2σ)

pressure (Torr)	k (s^{-1})	pressure (Torr)	k (s^{-1})
161	60.9(3.5)	1358	165.7(2.1)
204	63.8(2.8)	1489	167.8(4.7)
232	68.9(2.3)	1502	170.1(1.4)
250	81.9(3.3)	1608	175.3(4.5)
301	84.9(1.9)	1675	179.6(0.4)
349	85.0(2.1)	1763	182.2(3.8)
351	93.3(2.8)	1792	188.1(1.3)
400	97.8(2.4)	1938	192.1(1.7)
431	101.7(2.5)	2072	194.6(6.2)
472	103.4(2.1)	2400	196.9(1.3)
575	108.4(2.5)	2467	199.9(6.0)
607	118.6(1.9)	2586	202.1(1.3)
752	132.4(1.1)	3000	205.1(2.7)
796	139.2(2.7)	3462	213.8(2.1)
904	142.0(1.9)	3520	210.8(0.5)
919	138.2(1.8)	3646	215.7(1.3)
1020	140.9(1.7)	3785	212.8(2.2)
1041	153.1(2.1)	3965	214.5(1.9)
1089	147.1(2.5)	4268	213.9(3.7)
1114	152.1(2.8)	4632	212.9(2.2)
1135	156.4(2.2)	4896	216.9(2.2)
1267	160.0(1.9)	5236	216.0(2.1)

Rate constants were calculated using the program DNMR5,[28] which employs a nonlinear least-squares regression analysis to obtain the best fit of the experimental NMR spectrum. The program was provided with limiting chemical shifts, transverse relaxation times, and the digitized NMR spectrum. The limiting chemical shift difference was measured for slow exchange spectra at several temperatures and pressures and was found to be constant. Transverse relaxation times were obtained from measurement of the natural line width of [^{15}N]FA at slow and fast intramolecular exchange and TMS at pressures throughout the pressure region and interpolating to 333 K. T_2 values were observed to range from 0.42(0.12) s at 1020 Torr to 0.02(0.05) s at 250 Torr. Corrections for magnetic field inhomogeneity as determined from internal gaseous TMS and the line broadening were taken into account in the calculation of the T_2 value for each spectrum. At pressures of less than ~150 Torr, the T_2 contribution to the line shape could not be accurately determined. Possible effects on the rate constants due to wall collisions were discounted due to a previous study that reported this effect in methyl nitrite to be negligible at pressures above ~1 Torr.[8] Rate constants in the exchange region were obtained by iterating the rate constant, spectral origin, baseline height, and baseline tilt. All other parameters were held constant.

IR Spectroscopy. Gas-phase infrared spectra of [^{15}N]FA were measured at room temperature using a 7.5 cm long gas cell

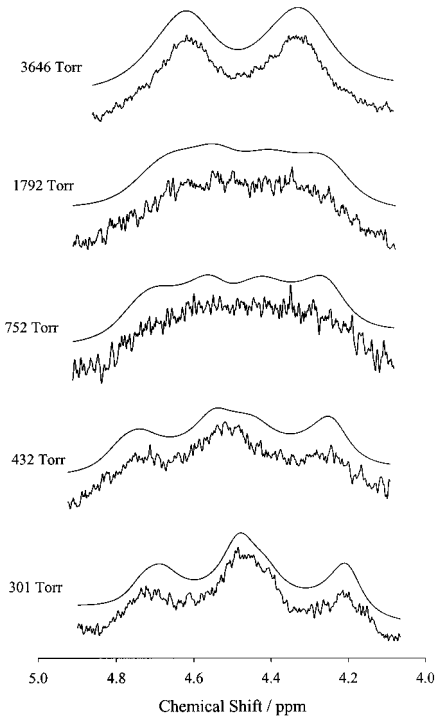

Figure 2. Pressure-dependent gas-phase NMR spectra of the amino proton region of [^{15}N]formamide at 333 K. The lower and upper traces correspond to experimental and simulated spectra, respectively. All samples contained 1.3 Torr of [^{15}N]formamide and 10−20 Torr of TMS. The listed pressures refer to the total pressure in each sample.

containing [^{15}N]FA at its vapor pressure and 400 Torr of SF_6 and a Galaxy Series 3000 FT-IR spectrometer with 1.0 cm^{-1} resolution to provide vibrational frequencies for use in RRKM calculations. Observed frequencies and assignments are listed in Table 2.

Ab Initio Molecular Orbital Calculations. Ab initio molecular orbital calculations were performed on Gateway microcomputers using the windows version of Gaussian 94.[29] Calculations were performed at the Hartree−Fock (HF) theory levels using the HF/6-311++G** basis set. Calculations (HF/6-31G**) were also performed for a FA−SF_6 dimer to estimate the interaction potential for use in kinetic modeling.

RRKM Calculations. Calculations were performed using the RRKM program written by Hase and Bunker[30] as well as the RRKM program from the UNIMOL program suite of Gilbert, Smith, and Jordan.[31] Weak collision effects were investigated using MAS55 also from the UNIMOL suite which calculates energy specific rate constants using an energy-grained master equation. Input parameters for the RRKM calculations are shown in Table 2.

Results

Experimentally determined and calculated pressure-dependent rate constants for FA internal rotation are described below.

Pressure-Dependent Rate Constants. Slow exchange spectra of [^{15}N]FA, obtained at 302.1 K, exhibit three broad resonances at 4.71, 4.49, and 4.21 ppm (amino protons) and a multiplet at 8.12 ppm (formyl proton).[1] Previously reported decoupling experiments demonstrated that the three broad resonances near 4.5 ppm arise from two overlapping doublets with a $^1J_{NH}$ of ca. 85 Hz.[1] Representative pressure-dependent gas-phase NMR spectra of the amino proton resonances of [^{15}N]FA at 333 K are shown in Figure 2 along with simulated spectra. All samples contained FA at its vapor pressure at 333 K which is estimated

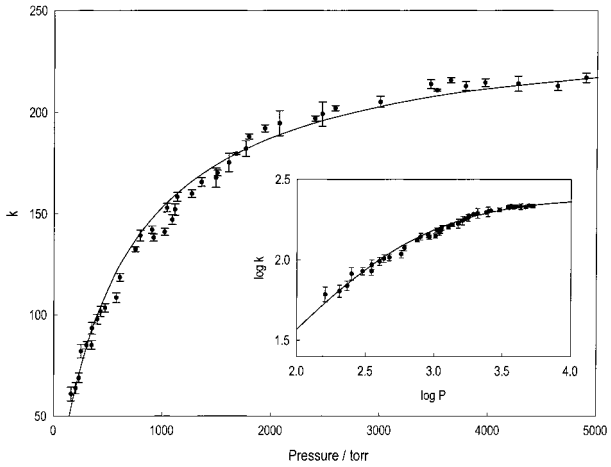

Figure 3. Pressure-dependent internal rotation rate constants for [^{15}N]-formamide at 333 K. The solid curve corresponds to rate constants calculated using RRKM theory and model parameters described in the text.

to be 1.3 Torr by comparison of sample and reference integration values, 10−20 Torr of TMS, and a variable partial pressures of SF_6. The pressures listed refer to the total pressure of each sample.[32] The calculated rate constants increase from 84.9(1.9) s^{-1} at 310 Torr to 215.7(1.3) s^{-1} at 3646 Torr.

Figure 3 shows pressure-dependent internal rotation rate constants of FA as a function of total sample pressure. Rate constants are also listed in Table 3. Forty-two rate constants were obtained at 333 K for total pressures ranging from 161 to 5236 Torr. The primary source of scatter in the experimental rate constants arises from sample preparation. At 333 K, the rate constants that were obtained ranged from 60.9 s^{-1} at 161 Torr to 216 s^{-1} at 5236 Torr. A pressure change of several orders of magnitude is required to observe the complete transition from unimolecular to bimolecular kinetics for most reactions. All the rate constants obtained in this study are in the unimolecular and intermediate falloff regions. Above 3000 Torr, the rate constants are almost independent of pressure. The lower pressure rate constants show a stronger pressure dependence and are in the falloff region. The RRKM calculations described below predict that the bimolecular region is at pressures below 10 Torr. It was not possible to obtain pressure-dependent rate constants below 150 Torr due to rapid spin−spin relaxation which caused severe line broadening and a poor signal/noise ratio. The location of the falloff on the pressure axis provides an estimate of the average energy specific rate constant for internal rotation of the activated FA molecules, $\langle k(E)\rangle$. At the pressure where the unimolecular rate constant is half of its high-pressure limiting value, around 600 Torr in this case, the collision deactivation frequency is equal to $\langle k(E)\rangle$.[6] Using a collision diameter of 4.8 Å, the collision deactivation frequency is ca. 5×10^9 at 600 Torr and 333 K.

RRKM Calculations. RRKM theory assumes that IVR in reacting molecules is ergodic and occurs at rate constants which exceed the RRKM rate constant for the process where activated molecules, in the absence of collisions, form the transition state.[6] Two transition states are possible for this process. Ab initio calculations at the HF/6-311++G** level predict that TS2 is 2.6 kcal mol^{-1} higher in energy than TS1. The contribution to the observed rate constant from a rotation path via TS2 is calculated to be less than 1% of the total rate constant. Only reaction via TS1 was considered in the final calculations described below.

When only the lower-energy tranistion state, TS1, is considered, the energy specific RRKM rate constant, $k_{RRKM}(E)$, is

$$k_{RRKM}(E) = \frac{LZ^{\ddagger}G^{\ddagger}(E - E_0)}{hZ\rho(E)} \qquad E > E_0 \qquad (1)$$

where E_0 is the critical energy, L is the statistical factor, $G^{\ddagger}(E - E_0)$ is the sum of the states in TS1, $\rho(E)$ is the density of states of the reactant, and h is Planck's constant.[6] $Z^{\ddagger}/Z$ is the ratio of the adiabatic partition functions which in this case are the rotational partition functions of TS1 and the ground state, excluding symmetry numbers. The concentration-dependent unimolecular rate constant is

$$k_{uni}[M] = \frac{L^{\ddagger}Z^{\ddagger}\exp(-E_0/kT)}{hZ}\int_{E_0}^{\infty}\frac{G^{\ddagger}(E - E_0)\exp(-E/kT)}{1 + k_{RRKM}(E)/k_2[M]}\,dE \qquad (2)$$

where $k_2[M]$ is the collision frequency.

The reactant $\rho(E)$ and Z values were calculated from experimental data. Since vibrational frequencies of [^{15}N]FA were not reported previously, they were measured in this study and are listed in Table 2. Assignments are based on analogy with the reported values for [^{14}N]FA.[33] HF/6-311++G** calculations best reproduced the experimental structure and vibrational frequencies of ground state FA, and this level of theory was used to calculate parameters for both transition states. HF/6-311++G** transition state vibrational frequencies multiplied by 0.893 were used to calculate $G^{\ddagger}(E - E_0)$. Since the experimental ground state rotational constants[34] are only ca. 2% smaller than those calculated at the HF/6-311++G** level, unscaled HF/6-311++G** rotational constants were used to calculate $Z^{\ddagger}$. $L^{\ddagger}$, the ratio of the rotational symmetry number of the reactant to that of the transition state, is 1 for FA internal rotation.[35] $G^{\ddagger}(E - E_0)$s, $\rho(E)$s, and $k_{RRKM}(E)$s were calculated at 71.4 cal mol^{-1} (25 cm^{-1}) increments from E_0 to E_0 + 14.3 kcal mol^{-1} (5000 cm^{-1}) using the direct count procedure.[36]

Calculated $G^{\ddagger}(E - E_0)$s, $\rho(E)$s, and $k_{RRKM}(E)$s and the relative population of activated FA molecules are plotted as a function of E^+ ($E^+ = E - E_0$) in Figure 4. In these calculations, the threshold energy, E_0, was 15.7 kcal mol^{-1}. A reactant molecule is "activated" when its internal energy equals or exceeds E_0. When $E_0 = 15.7$ kcal mol^{-1}, the average excess internal energy of activated FA molecules ($\langle E^+\rangle = \langle E - E_0\rangle$) is 0.80 kcal mol^{-1} at 333 K. Ninety-five percent of the activated FA molecules have energies within 1000 cm^{-1} of the barrier and undergo isomerization where the transition state vibrational state sum is 1 or 2. The average state density of activated FA molecules, $\langle\rho(E)\rangle$, is 7.2 states/cm^{-1}, and the average energy specific rate constant, $\langle k_{RRKM}(E)\rangle$, is 5.3 × 10^9 s^{-1}.

The falloff was calculated using a program written by Hase et al.[37] and also using the RRKM program from the UNIMOL program suite.[31] Using a Lennard-Jones (LJ) collision frequency instead of a hard sphere collision frequency has little effect on the shape of the strong collision falloff curve.[20] The critical energy, E_0, and collision diameter were varied to provide the best fit of the experimental falloff curve. The solid curve in Figure 3 corresponds to RRKM rate constants calculated using the input parameters described above, using a collision diameter, σ_{HS}, of 4.8 Å and a critical energy, E_0, of 15.68 kcal mol^{-1}.

An E_0 of 15.68 kcal mol^{-1} and a σ_{HS} of 4.8 Å are very reasonable for this system. The experimental E_∞, 16.6(0.3) kcal mol^{-1}, is consistent with an E_0 of 15.9 kcal mol^{-1}, assuming the average ground state and TS1 internal energies are the same and E_0 = 16.4 kcal mol^{-1} using average internal energies of the ground and TS1 calculated at the HF/6-311++G** level.[6] The most recent calculation at the CCSD(T) electron correlation level using a PVTZ basis set yielded a 15.8 kcal mol^{-1} barrier, excluding zero-point energy corrections.[2] Other recent reports estimate the barrier to be 15−16 kcal mol^{-1} (Table 4).[2,26,38−43] The diameter of FA is ca. 6 Å, using the molecular volume calculated at the 6-311++G** level, assuming spherical symmetry. The intermolecular potential for SF_6 has been determined from collision-induced light scattering spectra, viscosity measurements, and virial coefficient data, and σ has been reported to be between 4.6 and 5 Å and ϵ/k between 300 and 500 K.[44,45] Ab initio molecular orbital calculations of the energy of a FA−SF_6 collision complex as a function of the distance between the S atom and the point midway between the C and N atoms were performed at the HF/6-31G** level. Figure 5 shows the potential energy function for the minimum energy approach. Fitting this potential to the Lennard-Jones equation yields a well depth, ϵ/k, of 520 K and a σ_{LJ} of 4.02 Å. Averaging over all approach orientations would increase σ and reduce ϵ/k, due to contributions of less favorable approach angles.

Limited sample volatility necessitated the use of a bath gas for the pressure-dependent studies. SF_6 was chosen because of its volatility, high collision efficiency, and the lack of a proton signal. It is likely that the strong collision assumption is valid in this system for several reasons. The shape of the experimental

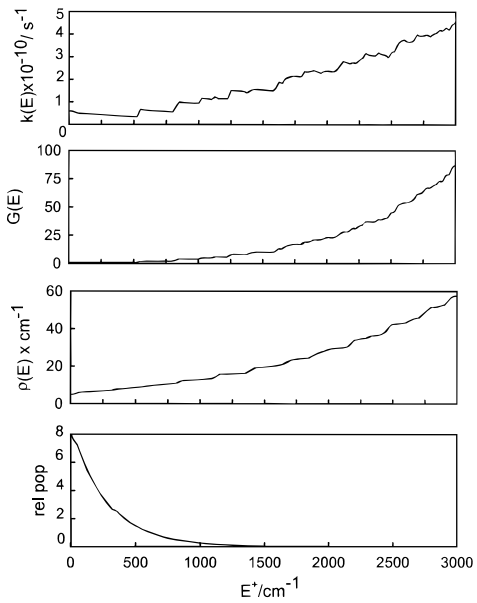

Figure 4. Properties of activated formamide molecules as a function of E^+ ($E^+ = E - E_0$, where E_0, the threshold energy, is 15.68 kcal mol^{-1}): (a) relative population at 333 K, (b) $\rho(E)$, state density, (c) $G(E)$ transition state sum, and (d) $k(E)$, energy specific RRKM rate constant.

TABLE 4: Theoretical Rotational Activation Energies (E_a, kcal mol^{-1}) to Internal Rotation in Isolated Formamide

method	E_a	ref
CCSD(T)/PVTZ	15.8	2
MP2/6-31G**	16.69	26
MP2/6-31G**	16.5	38
MP2/6-311++G**	15.89	39
HF/6-31G**	15.97	40
HF/6-31G**	15.98	41
MP2/CCDZP	15.5	42
HF/6-311G**	15.65	43
MP2/6-311G**	16.18	43
MP3/6-311G**	14.96	43
experiment	16.6(0.3)	1

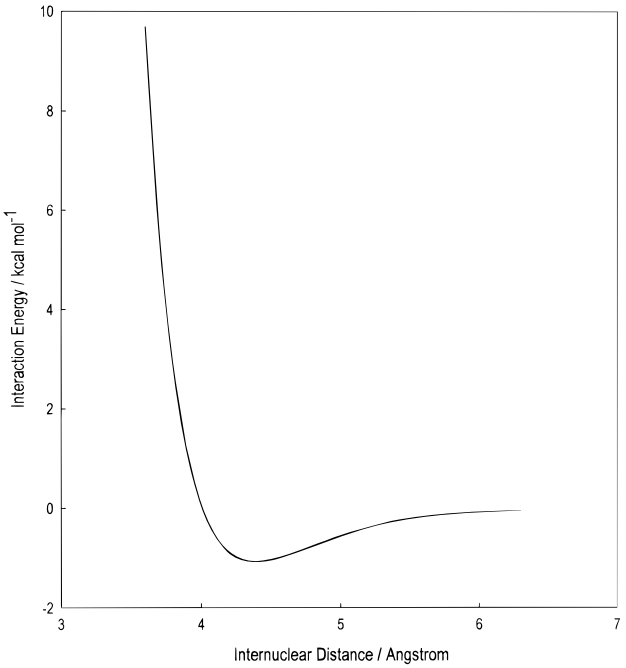

Figure 5. Interaction potential for the FA−SF_6 complex as a function of separation between the C−N bond of FA and the sulfur atom in SF_6. Calculations were performed at HF/6-31G** level of theory and with an increment step size of 0.1 Å. Lennard-Jones 12−6 potential fit parameters are as follows: $\epsilon/k = 520$ K and $\sigma_{LJ} = 4.02$ Å (reduced $\chi^2 = 0.84$).

falloff curve is reproduced by the standard RRKM calculation using the strong collision assumption for the deactivation step. The strong collision model assumes that collisional deactivation of activated molecules above the internal rotation barrier occurs in a single collision. This is reasonable because the average energy of activated FA molecules is ca. 280 cm^{-1} above the barrier and 95% of the activated population is within 1000 cm^{-1} of the barrier. The average energy transferred from an activated FA molecule to a bath molecule, $\langle \Delta E_{down} \rangle$, must be ca. 1000 cm^{-1} for the strong collision assumption to be valid. $\langle \Delta E_{down} \rangle$ is dependent on the size and complexity of the collision partners, and a value of 1000 cm^{-1} is not unreasonable.[46−48] It has been found that SF_6 is a strong collider for deactivating other molecules undergoing thermal chemical exchange processes at similar temperatures.[8,49] As a further check, additional calculations were performed using the weak collision model. The scatter in the experimental data does not allow a clear distinction between $\langle \Delta E_{down} \rangle$ values that differ by ca. 300 cm^{-1}. Satisfactory agreement between the shape of the observed and calculated falloff curves is also obtained using this model but only when $\langle \Delta E_{down} \rangle$ values of ca. $\geq$500 cm^{-1} are used.

The previously described calculations did not include any tunneling contribution to the rate constants. FA internal rotation involves hydrogen atom motion, and in principle, significant quantum mechanical tunneling can change the $k(E)$s and the location and curvature of the falloff curve.[6] The tunneling probability is dependent on the internal energy of the FA molecule and the shape of the potential energy surface near the top of the barrier. Tunneling effects were estimated using an Eckart potential.[50] The scaled imaginary frequency, 449 cm^{-1}, of TS1, calculated at the HF/6-311++G** theory level and a barrier height of 15.7 kcal mol^{-1} were used to parametrize the Eckart potential. Tunneling and reflectance probabilities as a function of internal energy were calculated. Because of this low vibrational frequency, quantum effects are small, with the probability of reaction changing from 0 to 1 between 14.75 and 16.5 kcal mol^{-1}. (Classically, the reaction probability is a step function which switches from 0 to 1 at the barrier.) The population distribution of the reacting molecules as a function of energy was calculated by multiplying the quantum mechanical probability function and the relative population distribution function calculated using direct count state densities from the RRKM program. At 333 K, the quantum corrected population distribution of reactive molecules is broader than the classical distribution, but the average energy of the reactive molecules, 16.3 kcal mol^{-1}, is only slightly lower than the classical value, 16.5 kcal mol^{-1}, calculated for the same barrier height. Approximately 60% of the reactive population is in the energy range between 14.75 and 16.5 kcal mol^{-1} where some tunneling perturbations may be expected, with ca. 20% being below the classical barrier. An estimate of possible tunneling effects on the distribution of energy specific rate constants and the shape of the falloff curve was obtained by calculating the tunneling corrections to the $k(E)$s using the method outlined by Miller.[51] In the nonclassical region between 14.75 and 16.5 kcal mol^{-1}, the average state density of a reacting molecule, $\langle \rho(E) \rangle$, is 4.8 states cm^{-1}, the average transition state sum $\langle G^{\ddagger}(E - E_0) \rangle$ is 0.3, and the average energy specific rate constant, $\langle k(E) \rangle$, is 1.6×10^9 s^{-1} when tunneling effects are included. In the classical limit, the lower range of reacting molecules is 15.7 kcal mol^{-1} and the corresponding average classical values for the energy range between 15.7 and 16.25 kcal mol^{-1} are as follows: $\langle \rho(E) \rangle = 5.9$ states cm^{-1}, $G^{\ddagger}(E - E_0) = 1.1$ states, and $\langle k(E) \rangle = 4.7 \times 10^9$ s^{-1}.

A tunneling-corrected RRKM model, requiring only a small decrease in the threshold energy, will also provide acceptable agreement with the pressure-dependent rate constants obtained in the study presented here. Lin et al. reported a study of methoxy radical decomposition where quantum effects were estimated to be much larger.[52] In that study, it also was impossible to distinguish between a classical and quantum-corrected RRKM model using experimental rate data.

Discussion

The observed pressure dependence of the internal rotation rate constants of FA between 161 and 5236 Torr is consistent with predictions of RRKM theory. Small deviations from statistical behavior would be undetectable in the experiments described here due to the quality of the experimental data, the insensitivity of RRKM calculations to some types of non-RRKM behavior, the uncertainty in parameters used in the RRKM calculations, and the uncertainty in the collision diameter. A previous study discussed in detail the effects of these uncertainties on drawing conclusions based on pressure-dependent rate constants for Berry pseudorotation of SF_4.[20] Large deviations from statistical kinetics such as found in studies of 2-fluoroethanol[24,25] and allyl fluoride[22,23] can be ruled out in the present case. For example, if the actual $\langle k(E) \rangle$ was 1 order of magnitude smaller than the RRKM-calculated $\langle k(E) \rangle$, the deactivating collision diameter required to keep $P_{1/2}$ at the experimentally measured value of ca. 600 Torr would be 1.5 Å which is unrealistically small.

The RRKM calculation which reproduces the experimental falloff curve yields an average energy specific rate constant, $\langle k(E) \rangle$, of 5.3×10^9 s^{-1}. This implies that IVR in activated FA molecules is ergodic and IVR lifetimes are ca. $\leq$200 ps. Also, for statistical kinetics, the average magnitude of the required coupling matrix elements between states near the internal rotation barrier of FA, $\langle H_{mn} \rangle$, estimated from the Fermi Golden Rule,

$$k_{IVR} = (4\pi^2/h)\rho(E)\langle H_{mn}\rangle^2 \quad (3)$$

must be ca. ≥ 0.1 cm^{-1}, assuming $\rho(E) = 7$ states/cm^{-1} and $k_{IVR} = 10^{10}$ s^{-1}. This time scale and coupling are not unreasonable. IVR lifetimes for FA molecules with energies in excess of that required for reaction have not been measured, but estimates may be made on the basis of studies of other molecules. IVR lifetimes for molecules initially excited into $\upsilon = 1$ of the C−H stretch are generally on the order of 1 ns,[53,54] 5 times longer than the average IVR lifetimes required for FA internal rotation to be statistical. These studies were usually performed in rotationally cooled beams. No general correlation with state density has been found in these experiments. There are several reasons to expect that IVR lifetimes may be shorter in this case. First, it is reasonable to assume that the anharmonic couplings between vibrational states of FA at energies near the internal rotation barrier, ca. 16 kcal mol^{-1}, will be larger than those between a C−H stretch and other nearly isoenergetic vibrational states at ca. 9 kcal mol^{-1}. In addition to having greater internal energy, the vibrational states of activated FA molecules are primarily combinations with quanta distributed among several modes. Second, the average J value for thermally equilibrated FA molecules at 333 K is 15, indicating that rotationally mediated vibrational coupling may be significant in activated FA molecules and a large manifold of K sublevels is available to participate in the redistribution process. Third, since FA has C_s symmetry, Coriolis interactions can occur between any two vibrations. Strong Coriolis interactions were observed between states of the torsion, out-of-plane NH_2, and the out-of-phase NCO−NH_2 bend, in the far-infrared spectrum of FA.[33] Also, the N−H stretch shows strong perturbations.[55] It is reasonable to assume that there will be similar strong coupling between other states with quanta in these modes which are close in energy. Finally, intermolecular interactions at the pressures used in the experiments described here should increase IVR rate constants from those observed in isolated molecules.

Internal rotation of FA has the smallest state density and shortest $\langle k(E)\rangle$ of the 15 conformational processes listed in Table 1. Agreement between observed and calculated pressure-dependent rate constants indicates that the kinetics of all these processes is statistical or nearly so. All the processes studied were thermally initiated, and the statistical requirement that $\langle k(E)\rangle$ is greater than k_{IVR} can be met with IVR rate constants which do not impose unrealistic or unphysical requirements on the IVR process. The most stringent IVR requirements are for FA since it has the fastest $\langle k(E)\rangle$.

The statistical nature of FA internal rotation is in contrast to results of studies where the initial state preparation was different. Allyl fluoride with an internal energy of 3100 cm^{-1}, initially in the asymmetric $=CH_2$ stretch, was found to have a conformer interconversion rate constant that is several orders of magnitude slower than predicted by RRKM theory.[22,23] A survival probability analysis determined that the IVR lifetimes of the initial ZOBS were 2 ns for the cis conformer and 90 ps for the gauche conformer. These values put an upper limit on the isomerization rate constants, 0.5×10^9 s^{-1} for the cis conformer and 1×10^{10} s^{-1} for the gauche conformer. RRKM theory predicts rate constants that are several orders of magnitude faster, a $k(E)$ of ca. 1×10^{12} s^{-1} for the cis conformer and 0.8×10^{12} s^{-1} for the gauche conformer. For 2-fluoroethanol, the energy of the ZOBS, 2980 cm^{-1}, is also about 3 times higher than the barrier to internal rotation.[24,25] The IVR lifetime of the ZOBS was 275 ps for the GG conformer. The measured and RRKM-calculated $k(E)$s were 3.7×10^{10} and 2.9×10^{12} s^{-1}, respectively. In both these cases, the RRKM-calculated $k(E)$ values are several orders of magnitude larger than the $\langle k(E)\rangle$ for FA isomerization primarily because the state sums are very large since the internal energy of the activated molecules was roughly 3 times the barrier height.

The different conclusions reached in the thermal and laser studies reflect the differences in the nature of the activated molecules. At the internal energies where the laser-initiated isomerizations occur, RRKM behavior requires IVR lifetimes 2 orders of magnitude shorter than those required for the thermally initiated internal rotation of FA. Besides the shorter IVR lifetimes required for statistical kinetics imposed by the experimental conditions, the initial excitation in the laser studies, exclusively in a stretching mode, is different than thermally activated FA internal rotation where most of the activated FA molecules have several quanta of energy in lower-frequency vibrational modes. The rotational state populations of the laser-initiated and thermal studies are very different. The initial ZOBS was prepared with a J of 0. The $J = 15$ state is the most populated rotational state of FA at 333 K.

A recent study of HOCl dissociation[56] found many states with nearly the same energy and/or J and K quantum numbers have dissociation rate constants which vary by more than 1 order of magnitude. The rate constants measured are also more than 3 orders of magnitude slower than those predicted by statistical theories. The unusual dissociation dynamics of this molecule was attributed to the nature of the initially prepared state that is only weakly coupled to the bath formed by most of the other vibrational states.

The statistical nature of FA internal rotation allows a direct comparison between experimental and calculated transition state parameters. High-level ab initio molecular orbital calculations successfully predicted gas-phase activation parameters for internal rotation of dimethylacetamide[57] and trifluoroacetamide.[4] In both studies, the experimental and calculated activation entropies, $\Delta S^{\ddagger}$, agree well. The temperature-dependent rate constants obtained previously for FA are consistent with a $\Delta G_{298}^{\ddagger}$ of 16.0(0.1) kcal mol^{-1}, a $\Delta H_{298}^{\ddagger}$ of 15.8(0.6) kcal mol^{-1}, and a $\Delta S_{298}^{\ddagger}$ of −0.7(0.9) cal mol^{-1} K^{-1}. The activation entropy, $\Delta S_{298}^{\ddagger}$, calculated at the HF/6-311++G** level for TS1 is −2.48 cal mol^{-1} K^{-1}. Vibrational frequencies calculated at the HF/6-311++G** level are typically ca. 10% greater than the experimental values. This is true for the higher vibrational frequencies of FA, but these calculations underestimate the inversion frequency in the ground state by 40%. The vibrational potential energy surface for the two out-of-plane NH vibrations calculated at the MP2 theory level was used to determine the fundamental vibrational frequencies for the torsion and inversion and was successful in reproducing the experimental values. $\Delta S_{298}^{\ddagger}$, calculated using the correct frequencies for these vibrations and appropriately scaled frequencies for the other vibrations of the ground state and transition state, is −1.50 cal mol^{-1} K^{-1}. This result demonstrates the failure of the harmonic approximation for the treatment of low-frequency large-amplitude vibrational motions. Agreement between experiment and theory is improved when the shape of the potential function is determined theoretically, and the vibrational frequencies are calculated using this potential. When the low-frequency vibrations are treated explicitly, structures and vibrational frequencies of transition states for simple conformational processes can be predicted with good accuracy with currently available computational methods.

Acknowledgment. We are pleased to acknowledge support from the National Science Foundation (Grant CHE 93-21079) and the University of California—Davis Committee on Research for support of this research. We also thank Dr. Andrzej Ozarowski for use of his computer program Crystal for generating molecular structures for Figure 1.

References and Notes

(1) Taha, A. N.; Neugebauer Crawford, S. M.; True, N. S. *J. Am. Chem. Soc.* **1998**, *120*, 1934.

(2) Fogarsi, G.; Szalay, P. G. *J. Phys. Chem. A* **1997**, *101*, 1400.

(3) Gas-phase NMR studies of N,N-dialkyl amides are summarized: (a) LeMaster, C. B. *Prog. Nucl. Magn. Reson. Spectrosc.* **1997**, *31*, 119. (b) True, N. S.; Suarez, C. *Advances in Molecular Structure Research*; JAI Press: New York, 1995; pp 115−155. (c) True, N. S. *Encyclopedia of NMR*; Grant, D. M., Harris, R. K., Eds.; John Wiley and Sons: Chichester, England, 1996; p 2173.

(4) LeMaster, C. L.; LeMaster, C. B.; True, N. S. *J. Am. Chem. Soc.* **1999**, *121*, 4478.

(5) See, for example: (a) *Conformational Behavior of Six-Membered Rings. Analysis, Dynamics, and Stereoelectronic Effects*; Juaristi, E., Ed.; VCH Publishers: New York, 1995. (b) *Dynamic Nuclear Magnetic Resonance Spectroscopy*; Jackman, L. M., Cotton, F. A., Eds.; Academic Press: New York, 1975.

(6) Holbrook, K. A.; Pilling, M. J.; Robertson, S. H. *Unimolecular Reactions*; John Wiley and Sons: Chichester, England, 1996.

(7) Hase, W. L.; Bunker, D. L. *J. Chem. Phys.* **1973**, *59*, 4621.

(8) Chauvel, J. P., Jr.; Friedman, B. R.; Van, H.; Winegar, E. D.; True, N. S. *J. Chem. Phys.* **1985**, *82*, 3996.

(9) Chauvel, J. P., Jr.; Conboy, C. B.; Chew, W. M.; Matson, G. B.; Spring, C. A.;

(10) Ross, B. D.; True, N. S. *J. Chem. Phys.* **1984**, *79*, 1469.

(11) Moreno, P. O.; True, N. S.; LeMaster, C. B. *J. Mol. Struct.* **1991**, *243*, 373.

(12) Ross, B. D.; True, N. S. *J. Am. Chem. Soc.* **1983**, *105*, 1382.

(13) Chu, P. S.; True, N. S. *J. Phys. Chem.* **1985**, *89*, 5613.

(14) Chu, P. S.; True, N. S. *J. Phys. Chem.* **1985**, *89*, 2625.

(15) LeMaster, C. B.; LeMaster, C. L.; Tafazzoli, M.; Suarez, C.; True, N. S. *J. Phys. Chem.* **1990**, *94*, 3461.

(16) LeMaster, C. B.; LeMaster, C. L.; Suarez, C.; Tafazzoli, M.; True, N. S. *J. Phys. Chem.* **1989**, *93*, 3993.

(17) LeMaster, C. B.; LeMaster, C. L.; Tafazzoli, M.; Suarez, C.; True, N. S. *J. Phys. Chem.* **1988**, *92*, 5933.

(18) Tafazzoli, M.; Suarez, C.; True, N. S.; LeMaster, C. B.; LeMaster, C. L. *J. Mol. Struct.* **1994**, *317*, 137.

(19) Tafazzoli, M.; Suarez, C.; True, N. S.; LeMaster, C. B.; LeMaster, C. L. *J. Phys. Chem.* **1992**, *96*, 10201.

(20) Spring, C. A.; True, N. S. *J. Am. Chem. Soc.* **1983**, *105*, 7231.

(21) Taha, A. N.; True, N. S.; LeMaster, C. B.; LeMaster, C. L.; Neugebauer-Crawford, S. M. *J. Phys. Chem. A* **2000**, *104* (15), 3341.

(22) Moreno, P. O.; Suarez, C.; Tafazzoli, M.; True, N. S.; LeMaster, C. B. *J. Phys. Chem.* **1992**, *96*, 10206.

(23) McWorter, D. A.; Pate, B. H. *J. Phys. Chem. A* **1998**, *102*, 8786.

(24) McWorter, D. A.; Pate, B. H. *J. Phys. Chem. A* **1998**, *102*, 8795.

(25) Green, D.; Hammond, S.; Keske, J.; Pate, B. H. *J. Chem. Phys.* **1999**, *110*, 1979.

(26) McWorter, D. A.; Hudspeth, E.; Pate, B. H. *J. Chem. Phys.* **1999**, *110*, 2000.

(27) Wiberg, K. B.; Breneman, C. M. *J. Am. Chem. Soc.* **1992**, *114*, 831.

(28) McCarthy, W. J.; Lapinski, L.; Nowak, M. J.; Adamowicz, L. *J. Chem. Phys.* **1998**, *108*, 10116.

(29) Stephenson, D. S.; Binsch, G. Program 365. *Quantum Chemistry Program Exchange*; Indiana University: Bloomington, IN. (b) LeMaster, C. B.; LeMaster, C. L.; True, N. S. Program 569 and QCMP059. *Quantum Chemistry Program Exchange*; Indiana University: Bloomington, IN.

(30) Frisch, M. J.; Trucks, G. W.; Schlegel, H. B.; Gill, P. M. W.; Johnson, B. G.; Robb, M. A.; Cheeseman, J. R.; Keith, T.; Petersson, G. A.; Montgomery, J. A.; Raghavachari, K.; Al-Laham, M. A.; Zakrzewski, V. G.; Ortiz, J. V.; Foresman, J. B.; Peng, C. Y.; Ayala, P. Y.; Chen, W.; Wong, M. W.; Andres, J. L.; Replogle, E. S.; Gomperts, R.; Martin, R. L.; Fox, D. J.; Binkley, J. S.; Defrees, D. J.; Baker, J.; Stewart, J. P.; Head-Gordon, M.; Gonzalez, C.; Pople, J. A. *Gaussian 94*, revision B.2; Gaussain, Inc.: Pittsburgh, PA, 1995.

(31) Hase, W. L.; Bunker, D. L. Program 234. *Quantum Chemistry Program Exchange*; Indiana University: Bloomington IN.

(32) Gilbert, R. G.; Smith, S. C.; Jordan, M. J. T. *UNIMOL program suite (calculation of falloff curves for unimolecular and recombination reactions)*; 1993 (available from the authors at School of Chemistry, Sydney University, NSW 2002, Australia or by e-mail to gilbert_r@summer.chem.su.oz.au).

(33) The pressures were measured at the filling temperature, ca. 298 K. The ideal gas law was used to calculate the pressures at 333 K.

(34) McNaughton, D.; Evans, C. J.; Lane, S.; Nielsen, C. J. *J. Mol. Spectrosc.* **1999**, *193*, 104.

(35) Hirota, E.; Sugisaki, R.; Nielsen, C. J.; Sorensen, O. *J. Mol. Spectrosc.* **1974**, *49*, 251.

(36) Pollak, E.; Pechukas, P. *J. Am. Chem. Soc.* **1978**, *100*, 2984. (b) Coulson, D. R. *J. Am. Chem. Soc.* **1978**, *100*, 2992.

(37) Holbrook, K. A.; Pilling, M. J.; Robertson, S. H. *Unimolecular Reactions*; John Wiley and Sons: Chichester, England, 1996; p 82.

(38) Hase, W. L. Private communication.

(39) Kienenger, M.; Suhai, S. *J. Mol. Struct.* **1996**, *375*, 181.

(40) Olsen, L. F.; Li, Y.; Houk, K. N.; Kresge, A. J.; Schaad, L. J. *J. Am. Chem. Soc.* **1995**, *117*, 2992.

(41) Laidig, K. E.; Cameron, L. M. *Can. J. Chem.* **1993**, *71*, 872.

(42) Burton, N. A.; Chiu, S. S.-L.; Davidson, M. M.; Green, D. V. S.; Hillier, I. H.; McDouall, J. J. W.; Vincent, M. A. *J. Chem. Soc., Faraday Trans.* **1993**, *89*, 2631.

(43) Wang, X.-C.; Facelli, J. C.; Simons, J. *Int. J. Quantum Chem.* **1993**, *42*, 123.

(44) Tsuzuki, S.; Tanabe, K. *J. Chem. Soc., Perkin Trans. 2.* **1991**, 1255.

(45) Meiander, N. *J. Chem. Phys.* **1993**, *99*, 8654.

(46) Aziz, R. A.; Slamam, M. J.; Taylor, W. L.; Hurly, J. J. *J. Chem. Phys.* **1991**, *94*, 1034.

(47) Gilbert, R. G.; Smith, S. C. *Theory of Unimolecular and Recombination Reactions*; Blackwell Scientific Publications: Oxford, England, 1990.

(48) Oref, I.; Tardy, D. C. *Chem. Rev.* **1990**, *90*, 1407.

(49) Tardy, D. C.; Rabinovitch, B. S. *Chem. Rev.* **1977**, *77*, 369.

(50) Moreno, P. O.; True, N. S. *J. Chem. Phys.* **1991**, *95*, 57.

(51) Johnston, H. S. *Gas-Phase Reaction Rate Theory*; Ronald Press Co.: New York, 1966; pp 37−47.

(52) Miller, W. H. *J. Am. Chem. Soc.* **1979**, *101*, 6810.

(53) Page, M.; Lin, M. C.; He, Y.; Choudbury, T. K. *J. Chem. Phys.* **1989**, *91*, 4404.

(54) Flynn, G. W.; Parmenter, C. S.; Wodtke, A. M. *J. Phys. Chem.* **1996**, *100*, 12817.

(55) Nesbitt, D. J.; Field, R. W. *J. Phys. Chem.* **1996**, *100*, 12735.

(56) Brummer, C. L.; Shen, M.; Hewett, K. B.; Philips, L. A. *J. Opt. Soc. Am.* **1994**, *B11*, 176.

(57) Calllegari, A.; Rebstein, J.; Jost, R.; Rizzo, T. R. *J. Chem. Phys.* **1999**, *111*, 7359.

(58) Wiberg, K. B.; Rablen, P. R.; Rush, D. J.; Keith, T. A. *J. Am. Chem. Soc.* **1995**, *117*, 4261.